Co-published by
Institute of Fluid-Flow Machinery
Polish Academy of Sciences
Committee on Thermodynamics and Combustion
Polish Academy of Sciences

http://www.imp.gda.pl/archives-of-thermodynamics/

Modelling the heat transfer of nanofluid towards a radiating stretching sheet of varying thickness using thermal flux

Pragya Pandey[a], Dhatchana Moorthy Kavitha[b*], Thangaraju Lawanya[b]

[a]Department of Mathematics, SRM Institute of Science and Technology, Ramapuram, Chennai – 600 089, Tamil Nadu, India
[b]Department of Mathematics, Saveetha School of Engineering, Saveetha Institute of Medical and Technical Sciences, Saveetha Nagar, Thandalam, Chennai – 602 105, Tamil Nadu, India
Corresponding author email: soundarkavitha@gmail.com

Received: 10.06.2024; revised: 21.08.2024; accepted: 03.10.2024

Abstract

The present paper targets the flow of fluid with Fe_3O_4 particles as nanomaterial over a non-linear elongated sheet with changing width. The process holds vital importance in various industries like paper manufacturing, extrusion of dyes and filaments, atomic reactors and many more. Nanofluids depict special features which give them the potential to be also used in power engines, refrigerators, power plants as well as pharmaceutical processes. Hence, the presented model is designed to intensify the rate of heat transfer and to reduce energy wastage, and tailor for the optimal selection of parameters like conductivity as well as viscosity, which will improve the effectiveness of the heat transfer process. The main idea behind this investigation is to calculate the effect of electromagnetohydrodynamics, Biot number, Eckert number, radiation along with the absorption factor. In this paper, the flow is modelled by using Navier-Stokes equations which are customised to Prandtl boundary layer equations. The Adams-Bashforth predictor-corrector is used to obtain numerical solutions. The present study helps to potentially improve and achieve the desired quality of the stretching sheet. Moreover, a negligible amount of activation energy is required, finding an economical way to get suitable outputs.

Keywords: Nanofluid; Nanoparticles; Stretching sheet; Thermal radiation; Viscosity; Electromagnetohydrodynamics

Vol. 46(2025), No. 2, 83–91; doi: 10.24425/ather.2025.154908

Cite this manuscript as: Pandey, P., Kavitha, D.M, & Lawanya, T. (2025). Modelling the heat transfer of nanofluid towards a radiating stretching sheet of varying thickness using thermal flux. *Archives of Thermodynamics*, 46(2), 83–91.

1. Introduction

Engineers in the domain of computational fluid dynamics (CFD) are curious to explore the cooling mechanism of elongated sheet due to its wide variety of practical importance. In many factories, different domains have utilized the cooling of stretching sheets to obtain the desired quality of the sheet. Although many liquids have been tried as cooling agents, nanofluids have been found superior in comparison to all other fluids. The fluid flow over this type of sheet has many uses in industrial processes like manufacturing parts of aircrafts, extraction of fibres from glass, manufacturing of polymer sheets, drawing filaments and dyes, and many more. The quality of sheets relies upon on rate of cooling as well as heat removal. Many scientists studied the mechanism of action of nanofluids in various geometrical shapes. In [1], copper nanofluids flow over an elongated sheet is explored. An exact solution of a thin fluid layer flowing over a stretching sheet was found in [2]. The combination of dust particles mixed

Nomenclature

A – variable viscosity parameter
A^* – space-dependent coefficient
b – stretching constant
B, B_o – magnetic field strength, T
B^* – time-dependent coefficient
Bi – Biot number
c – stretching parameter
C_p – heat capacity, J kg^{-1} K^{-1}
E, E_0 – electric field strength, N C^{-1}
E_1 – electric field parameter
Ec – Eckert number
f – base fluid
f' – velocity parameter
h – step size
k – kth iteration
k^* – mean absorption coefficient
M – magnetic field parameter
n – parameter of velocity power index
N – coefficient related to stretching sheet
Nu – Nusselt number
Pr – Prandtl number
q''' – non-uniform flux
qr – radiative heat flux, W m^{-2}
Rd – parameter of radiation
T – fluid temperature, K
T_∞ – free stream temperature, K
U_w – wall velocity, m s^{-1}
u, v – components of velocity along x- and y-axis, m s^{-1}
x, y – Cartesian coordinates, m

Greek symbols

α – wall thickness parameter
ε – infinitesimal small
η – non-dimensional similarity variable
θ – dimensionless temperature
ϑ – viscosity parameter
κ – thermal conductivity, W m^{-1} K^{-1}
μ – dynamic viscosity, kg m^{-1} s^{-1}
ν – kinematic viscosity, m^2 s^{-1}
ρ – density, kg m^{-3}
σ – electric conductivity, S m^{-1}
σ^* – Stefan-Boltzmann constant, W m^{-2} K^{-4}
ϕ – volume fraction
ψ – streamline function

Subscripts and Superscripts

f – base fluid
nf – nanofluid
t – tri
p – particle
s – solid
w – wall
' – differentiation with respect to η

Abbreviations and Acronyms

FEM – finite element method
EMHD – electromagnetohydrodynamics
MHD – magnetohydrodynamics

with nanoparticles flowing over a stretched plate was investigated with novel mathematical modelling in [3]. The flow induced by nanofluid over an exponentially stretchable plate was surveyed in [4] by considering the impact of viscous dissipation. The thermophysical characteristics of nanofluid flow along a vertical plate due to porous media along tiny sized suspensions were studied with a novel method in [5]. The situation dealing with free convection inside a cavity taking into account nanoparticles dispersed in the base fluid was solved numerically in [6]. The impact of dust grains dispersed on a stretched surface was investigated in [7]. The process of dispersing particles in liquids over an increasingly stretching sheet was studied and framed in [8] with viscous dissipation and magnetohydrodynamics (MHD) taken into account. The comparison of heat transfer in a normal fluid and nanofluid flow using different nanoparticles on a stretching surface was studied in [9]. The nanoparticle's shape was examined in [10] at a point of the magneto stagnation flow with a dual combination of effects of chemical reaction and thermal radiation. A 3D modelling of magneto flow of nanofluids over a disc was presented in [11]. The Casson flow stimulated due to gyrotactic microbes in a conical shape was solved using the Homotopy Analysis Method (HAM). Lately, the impact of magnetic nanofluid over a moving disc was deducted in [12]. The impact of MHD on nanofluid flow over an inclined stretched plate bearing an unsteady thin film flow was examined in [13].

MHD flow in nanofluids has attracted attention due to its extraordinary potential to control the rate of heat transfer. Magnetohydrodynamics is mainly derived from 3 terms: magneto, hydro and dynamics – the term was coined in [14]. The process of flow with magnetohydrodynamics on a stretched plate up to a stagnation point was investigated in [15] and estimated numerically using the finite difference method. Buongiorno's model was considered as a base to study MHD flow of nanofluid over an extending plate taking the slip factor into account [16]. A case of bidirectional MHD flow of nanofluid with Hall current and heat flux over a stretching sheet was solved by [17]. It was noticed that Hall current and heat flux boosted the quality of the sheet. Many studies related to MHD are utilized in improving machine efficiency [18–20] and serve as the motivation for the current effort. Additionally, it is noted that studies on heat transfer have utilized linear extending sheets. To document the impact of electromagnetohydrodynamic (EMHD), a non-linear elastic sheet of varying thickness has also been incorporated with boundary-layer flow of a nanofluid. Changing width of stretching sheets holds actual uses in industries, including appliance constructions and patterns, nuclear reactor mechanisation, filament extrusion, paper industry and several other fields [21–24]. Velocity slip along ternary nanofluid over a stretching sheet was enquired in [25] and concluded that the inclusion of three

different nanoparticles accelerated the conduction of heat. Hybrid nanofluid over a porous stretched sheet was investigated in [26]. Natural convection of hybrid nanofluid in a quadrantal enclosure was studied in [27]. The study signified the role of magnetic field in the process of heat removal. The process was investigated by taking equal proportions of water and ethyl glycol. The dual effect of two particle nanofluid and magnetic field was analysed in [28–29]. Radiating hybrid nanofluid flow with the Hall effect over a stretching/shrinking sheet was scrutinised in [29]. Statistical modelling of radiative hybrid nanofluid was meticulously solved in [30]. Darcy-Forchheimer flow of hybrid nanofluids with melting heat transfer over a porous rotating disk was investigated in [31]. Gyrotactic and heat transfer of water with MHD taking single-walled carbon nanotubes (SWCNT) as nanoparticles was studied in [32].

This study aims to provide new horizons to the effects of heat transfer using iron oxide nanofluid, which is cost-effective over a non-linear stretching sheet with changing width. The effects of thermal radiation, changing heat flux, viscous dissipation, electromagnetohydrodynamics and ohmic heating are taken into account. Furthermore, the effects of Nusselt number and skin friction coefficient have been calculated. This study is significant to obtain better quality of a stretching sheet which holds vital industrial importance, and it proves to be another milestone in the computational fluid dynamic in the field of nanofluids.

2. Methods and materials

A two-dimensional nanofluid with water as a base is made to flow over a stretching sheet of changing thickness. The nature of sheet is non-linear (Fig. 1). The velocity of fluid is given by $U_w(x) = b(x + c)^n$ [33], where b is a constant, c is the extending parameter and n is the exponential parameter. The direction along the stretching plate is considered an x axis. The EMHD force is considered to act along a y axis. The variation of thickness is taken as $y = N(x + c)(1 - n)/2$. It is assumed that the pressure difference does not alter the length of the sheet. N is taken as a minor factor for this purpose. The application of two forces of equal magnitude and opposite direction leads to the elongation of the plate through its slit.

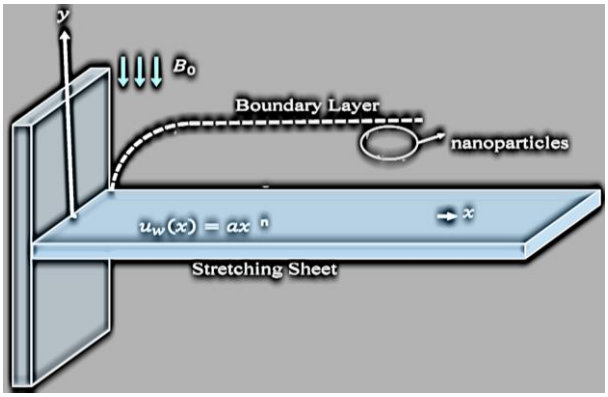

Fig. 1. Three different boundary layers.

In order to maintain the Reynolds number in a low range, electric and magnetic fields are applied perpendicular to the flow direction. The mathematical transformations for electric and magnetic fields can be formulated as $E(x) = E_0(x + c)^{\frac{n-1}{2}}$ and $B(x) = B_0(x + c)^{\frac{n-1}{2}}$, [17], respectively. The temperature difference due to layers of fluids is assumed to be zero. Furthermore, the effects of non-uniform heat flux, viscous dissipation, and Joule heating are incorporated with Prandtl's boundary layer equations:

$$\frac{\partial u}{\partial x} + \frac{\partial v}{\partial y} = 0, \tag{1}$$

$$\rho_{nf}\left(u\frac{\partial u}{\partial x} + v\frac{\partial u}{\partial y}\right) = \frac{\partial}{\partial y}[\mu(T)] + \frac{\sigma_{tnf}B_0{}^2u}{\rho_{tnf}} + \\ + \sigma_{nf}[E(x)B(x) - B(x)^2u], \tag{2}$$

$$\left(\rho C_p\right)_{nf}\left(u\frac{\partial T}{\partial x} + v\frac{\partial T}{\partial y}\right) = k_{nf}\frac{\partial^2 T}{\partial y^2} + \\ + \frac{16\sigma^*}{3k^*}\frac{\partial^2 T}{\partial y^2} + \mu_{nf}\left(\frac{\partial u}{\partial y}\right)^2 + q''' + \sigma_{nf}[uB(x) - E(x)]^2, \tag{3}$$

using boundary conditions represented by the equations:

$$u = U_w(x) = (x + c)^n,\ y = 0,$$

$$-k\frac{\partial T}{\partial y} = h(T_w - T) \quad \text{at} \quad y = N(x + c)^{\frac{n-1}{2}} \quad \text{and} \tag{4}$$

$$u \to 0, \quad T \to T_\infty \ \text{ as } \ y \to \infty,$$

where the components of speed along coordinate axes are represented by u and v; T is the temperature fluid temperature, ρ_{nf} is the density, σ_{nf} is the measure of electrical conduction, $\alpha_{nf} = \frac{k_{nf}}{(\rho C_p)_{nf}}$ is the thermal diffusivity, σ^* symbolises the Stefan-Boltzmann constant and k^* symbolises the average value of absorption. The coefficient of viscosity [16] is tailored by the equation:

$$\mu(T) = \mu^*[a_1 + b_1(1 - \theta)(T_w - T_\infty)], \tag{5}$$

where μ^* is a standard reference viscosity, whereas a_1, b_1 are assumed to be constants. q''' that appears in Eq. (3) is the non-uniform value of heat flux and is computed by:

$$q''' = \frac{k_{nf}U_w(x)}{v_f(x+c)}[A^*(T_w - T_\infty) + B^*(T - T_\infty)], \tag{6}$$

where A^* and B^* are heat generation and absorption parameters, respectively.

2.1. Conversion of equations

To solve the given partial differential equations, it is necessary to introduce the following dimensionless variables:

$$\psi = (b\,\vartheta_{nf})^{\frac{1}{2}}xf(\eta), \tag{7}$$

$$\eta = \left[\frac{(n+1)b(x+c)^{n-1}}{2\vartheta}\right]^{\frac{1}{2}}y, \tag{8}$$

$$u = b(x + c)^n f'(\eta), \tag{9}$$

$$v = -\left[\frac{(n+1)b(x+c)^{n-1}}{\vartheta}\right]^{\frac{1}{2}}\left[f(\eta) + \eta f'(\eta)\frac{n-1}{n+1}\right], \quad (10)$$

$$T = T_w(x), \quad (11)$$

where $\psi(x,y)$ is the streamline function and $u = \frac{\partial\psi}{\partial y}$ and $v = -\frac{\partial\psi}{\partial x}$, η is a similarity variable, and the temperature is non-dimensionlised as follows:

$$\theta(\eta) = \frac{T-T_\infty}{T_w-T_\infty}. \quad (12)$$

It is necessary to convert the partial differential formulas to ordinary differential equations:

$$A_0\{[a_1 + A(1-\theta)]f''' - A\theta' f''\} +$$
$$+A_1\left(f'''f - \frac{2n}{n+1}f'^2\right) + A_2M(E_1 - f') = 0. \quad (13)$$

$$\theta''\left(A_4 + \frac{4}{3}\mathrm{Rd}\right) + \mathrm{Pr}\left[A_0\mathrm{Ec}f''^2 + A_2\mathrm{Ec}M(f'-E_1)^2 + \right.$$
$$\left.+A_3 f\theta' - A_3 f'\theta\left(\frac{1-n}{1+n}\right)\right] + A_4\frac{2}{n+1}(Af' + B\theta) = 0. \quad (14)$$

where the prime (′) denotes differentiation concerning η and

$$f(\eta) = \left(\frac{1-n}{1+n}\right)\alpha, \qquad f'(\eta) = 1,$$
$$\theta'(\eta) = -\mathrm{Bi}[1-\theta(0)] \text{ at } \eta = 0;$$
$$f'(\eta) = 0, \qquad \theta(\eta) = 0 \quad \text{as} \quad \eta \to \infty.$$

The non-dimensional parameters are given by:

$$M = \frac{2\sigma_f B_0^2}{\rho_f b(n+1)}, \qquad E_1 = \frac{E_0}{B_0 b(x+c)^n},$$

$$\mathrm{Rd} = \frac{4\sigma T_\infty^3}{kk_f}, \qquad \mathrm{Ec} = \frac{b^{2(x+c)^2}}{(C_p)_f(T_w-T_\infty)},$$

$$\mathrm{Pr} = \frac{\vartheta_f(C_p)_f}{k_f}, \qquad \alpha = N\left(\frac{b(n+1)}{2\vartheta_f}\right)^{\frac{1}{2}},$$

$$\mathrm{Bi} = \frac{h}{k_f}\left[\frac{2\vartheta_f(x+c)}{b(n+1)}\right]^{1-n}, \quad A = b_1(T_w - T_\infty),$$

where M symbolises magnetic field intensity, E_1 − magnitude of electric field, Rd − radiation parameter, Pr represents the Prandtl number, Ec is the Eckert number, α − wall thickness, Bi − Biot number, A_0, A_1,. A_2, A_3 and A_4 are unknown constants (dimensionless coefficients).

2.2. Thermophysical properties of nanofluid

To calculate fixed values, the thermophysical properties of water and iron oxide are presented in Table 1.

The volume fraction ϕ of nanoparticles determines the heat capacity, thermal conductivity and viscosity of the nanofluids. The nanofluid's effective density is given by

$$\rho_{nf} = (1-\phi)\rho_f + \phi\rho_s \quad (15)$$

and the heat capacitance of nanofluid by

$$(\rho C_p)_{nf} = (1-\phi)(\rho C_p)_f + \phi(\rho C_p)_s. \quad (16)$$

According to Brinkman [34], the dynamic viscosity of a nanofluid is as below:

$$\mu_{nf} = \frac{\mu_f}{(1-\phi)^{2.5}}, \quad (17)$$

$$\frac{k_{nf}}{K_f} = \frac{(k_s+2k_f)-2\phi\,(k_f-k_s)}{(k_s+2k_f)+\phi\,(k_f-k_s)}. \quad (18)$$

The electrical conductivity of a nanofluid can be given by

$$\sigma_{nf} = 1 + \frac{3\phi\left(\frac{\sigma_p}{\sigma_f}-1\right)}{\left(\frac{\sigma_p}{\sigma_f}+2\right)-\left(\frac{\sigma_p}{\sigma_f}-1\right)\phi}\sigma_f. \quad (19)$$

2.3. Skin friction coefficient

The skin friction coefficient C_f can be derived from

$$C_f = \frac{\tau_w}{\rho_f U_w^2},$$

where $\tau_w = \mu_{nf}\left(\frac{\partial u}{\partial x}\right)_{y=N(x+c)^{\frac{n-1}{2}}}$. Using the above equations, we get

$$C_f\mathrm{Re}_x^{\frac{1}{2}} = \frac{A_0}{A_4}\left(\frac{n+1}{2}\right)^{\frac{1}{2}}f'(0). \quad (20)$$

2.4 Nusselt number

The concept of the Nusselt number can be modified for nanofluids. The Nusselt number for nanofluids is given by:

$$\mathrm{Nu} = \frac{(x+c)q_w}{k_f(T_w-T_f)},$$

where $q_w = -k_{nf}\left(\frac{\partial T}{\partial y}\right)_{y=N(x+c)^{\frac{n-1}{2}}}$. Using the above we get

$$\mathrm{NuRe}_x^{\frac{1}{2}} = -A_4\left(\frac{n+1}{2}\right)^{\frac{1}{2}}\theta'(0). \quad (21)$$

2.5. Solution of the problem

Numerical methods are efficient tools to deal with non-homogeneous equations with higher order accuracy. The system of nonlinear ordinary differential equations (ODE) is converted into 5 linear equations. The Adams-Bashforth predictor-corrector method was utilized to fetch the solution. It is a linear multistep methodology, which helps our results to be more accurate by utilizing the quantitative value of the last step.

The calculation works can be divided into two phases, first to get appropriate values as a predictor and the Adams-Moulton method to get a corrector.

The first order system for $\theta(\eta)$ and $f(\eta)$ is as follows:

$$g_1 = f', \quad g_2 = g_1', \quad g_3 = g_2', \quad (22)$$

$$g_3 = g_2' = \frac{1}{[a_1+A(1-\theta)]}\left[A\,\theta_1 f_2 - \frac{B_1}{B_0}\left(g^2 f - \frac{2}{n+1} g_1^2\right) - \frac{B_2}{B} M(E_1 - g_1)\right], \quad (23)$$

$$\theta_1 = \theta', \quad \theta_2 = \theta_1', \quad (24)$$

$$\theta_2 = \theta_1' = \frac{1}{1+\frac{4}{3}\mathrm{Rd}}\left\{\Pr\left[\frac{B_0}{B_4}\mathrm{Ec} f_2^2 + \frac{B_2}{B_4}\mathrm{Ec} M(E_1 - g_1)^2 + \frac{B_3}{B} f\theta_1\left(\frac{1-n}{1+n}\right)\right]\right\}. \quad (25)$$

Along with the boundary conditions

$$f(\eta) = \left(\frac{1-n}{1+n}\right)\alpha, \quad f'(\eta) = 1, \quad \theta'(\eta) = -\mathrm{Bi}[1-\theta(0)] \text{ at } \eta = 1 \quad (26)$$

$$f'(\eta) = 0, \quad \theta(\eta) = 0 \text{ as } \eta \to \infty$$

where:

$$B_0 = \frac{\mu_{nf}}{\mu_f} = \frac{1}{(1-\phi)^{2.5}}, \quad (27)$$

$$B_1 = \frac{\rho_{nf}}{\rho_f} = (1-\phi)\rho_f + \phi\frac{\rho_p}{\rho_f}, \quad (28)$$

$$B_2 = \frac{\sigma_{nf}}{\sigma_f} = 1 + \frac{3\phi\left(\frac{\sigma_p}{\sigma_p}-1\right)}{\left(\frac{\sigma_p}{\sigma_f}+2\right)-\left(\frac{\sigma_p}{\sigma_p}-1\right)\phi}, \quad (29)$$

$$B_3 = \frac{(\rho C_p)_{nf}}{(\rho C_p)_f} = (1-\phi) + \phi\frac{(\rho C_p)_s}{(\rho C_p)_f}, \quad (30)$$

$$B_4 = \frac{k_{nf}}{K_f} = \frac{(k_s+2k_f)-2\phi\,(k_f-k_s)}{(k_s+2k_f)+\phi\,(k_f-k_s)}. \quad (31)$$

Initial values are obtained with the help of the 4th order Runge-Kutta method. Afterwards, the explicit fourth order predictor is given by the formula:

$$y_{n+1,corr} = y_n + \frac{1}{24}(9y'_{n+1} - 59y'_n + 37y'_{n-1} - 9y'_{n-2}). \quad (32)$$

The final values of $f'(u,b)$ (ambient velocity calculated by predictor) are calculated from Eq. (32) by subtracting from boundary values. A similar methodology is used to fetch $\theta(u,b)$ (ambient temperature calculated by the predictor). If results are larger than ε, then initial guesses are changed and the secant method is employed for making another guess. The process is repeated until we get the similarity variable. The value of the similarity variable is assumed from 0 to ∞, η_0 represents the initial value of the similarity variable, however, the solution converges by assigning its value up to 5.

The differential operator is defined by Eqs. (33) and (34):

$$\frac{df}{d\eta} = q(\eta, f), \quad f(\eta_0) = f_0, \quad (33)$$

$$\frac{d\theta}{d\eta} = q(\eta, \theta), \quad \theta(\eta_0) = \theta_0. \quad (34)$$

The formula for the Adams-Bashforth predictor approach is given by Eqs. (35) and (36):

$$f_{k+1} = f_k + \frac{3h}{2}q(\eta_k, f_k) - \frac{h}{2}q(\eta_{k-1}, f_{k-1}), \quad (35)$$

$$\theta_{k+1} = \theta_k + \frac{3h}{2}q(\eta_k, \theta_k) - \frac{h}{2}q(\eta_{k-1}, \theta_{k-1}). \quad (36)$$

whereas the Adams-Moulton formula by Eqs. (37) and (38):

$$f_{k+1} = f_k + \frac{h}{2}q(\eta_{k+1}, f_{k+1}) - \frac{h}{2}q(\eta_k, f_k), \quad (37)$$

$$\theta_{k+1} = \theta_k + \frac{h}{2}q(\eta_{k+1}, \theta_{k+1}) - \frac{h}{2}q(\eta_k, \theta_k), \quad (38)$$

where h is the step size. The obtained results were verified and compared with the previous analysis.

3. Analysis of results

The effects of various thermophysical parameters are shown by suitable graphs. The quantities considered are heat generation or absorption factor, the wall thickness, electric and magnetic field factors and viscous dissipation. Table 2 is designed to match the outputs with earlier studies. The results obtained are in perfect match with the earlier analyses.

Figure 2 shows the influence of n on the temperature and velocity profile. The velocity shoots up as the value of n increases, resulting in more fluid to be displaced and hence increasing in the velocity associated with the boundary layer. The increase in velocity ultimately lowers the heat transfer rate.

The velocity is decreased when the fluid is closer to the sheet, resulting in reduction of the boundary layer. Because of the wall thickness parameter, the temperature gradient similarly demonstrates a downfall. Figure 3 guides the importance of incorporation of magnetic factor which influences both the temperature gradient and speed. Increasing the magnetic field reduces the nanofluid flow. This is expected as an increasing value of the MHD parameter of electrically charged nanoparticles results in an increase of the Lorentz force, a force which retards the motion of fluid. This property is useful to fetch the desired velocity. The graph shows that the magnetic field is inversely related to the velocity factor.

Figure 4 exhibits the role of viscous dissipation in the temperature profile. The Eckert number shows a relation between the kinetic energy of nanofluid flow and the enthalpy difference between the surrounding area and the wall to represent the heat dissipation. This is in alignment with the study conducted in [8] in the absence of magnetic field. The dimensionless temperature for various Rd values is also displayed in Fig. 4. The radiation parameter is designed to detect the rate of heat transfer. An increase in radiation accelerates the amount of heat transfer which leads to an increase in boundary layer thickness. Therefore, both the temperature gradient and boundary layer thickness assume higher values with the increasing Rd. The radiation effect is designed to customize the fluid velocity.

Table 2. Thermophysical parameters.

Pr	Gul et al. [8]	Saeed et al. [9]	Present study
2.0	0.9113	0.9114	0.9110
6.2	1.5797	1.5796	1.5786
7.0	1.8954	1.8954	1.8964
20.0	1.3539	1.3539	1.3539

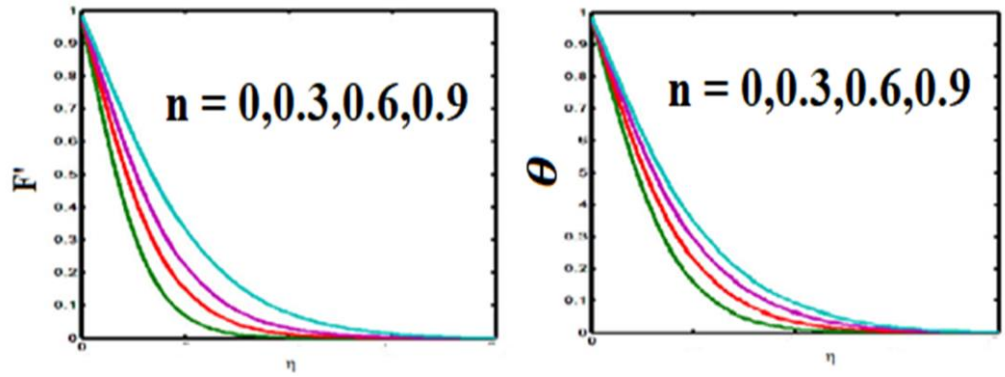

a) b)

Fig. 2. Effect of *n* on velocity (a) and temperature (b).

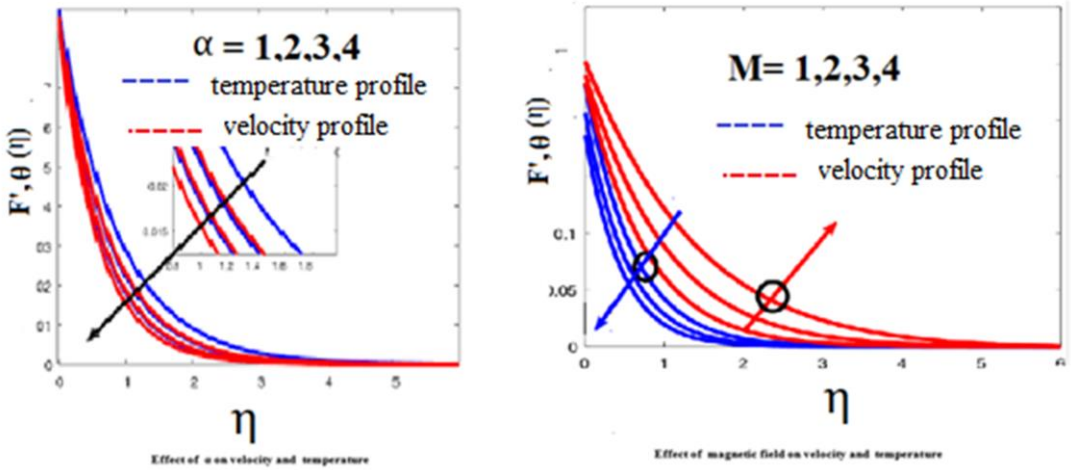

Fig. 3. The effect of magnetic field on velocity and temperature.

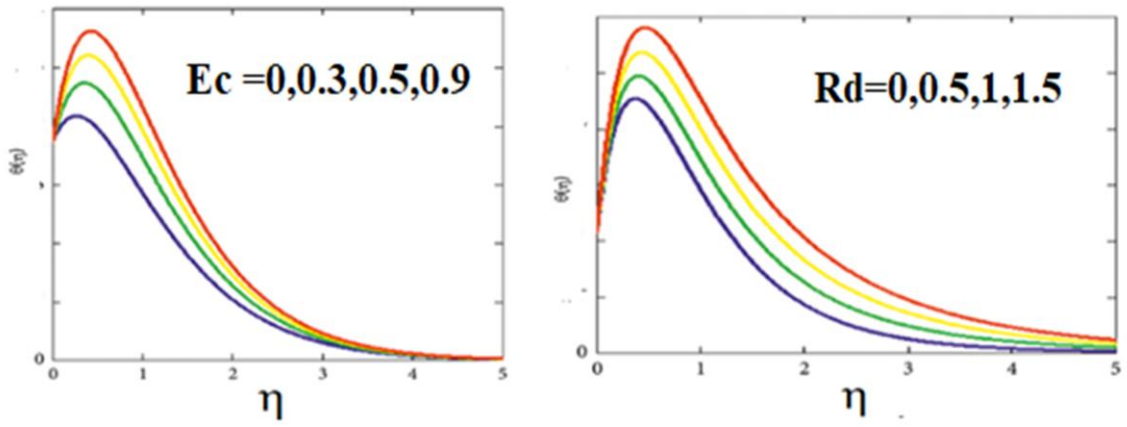

Fig. 4. Influence of Eckert number and radiation parameter on temperature.

Figure 5 illustrates the effect of Biot number (Bi). The Biot number, which represents the ratio of convective heat transfer to conductive heat transfer, significantly influences the thermal boundary conditions. As observed, increasing the Biot number leads to a higher temperature gradient near the surface, indicating enhanced heat transfer at the boundary. This result shows an excellent agreement with [9].

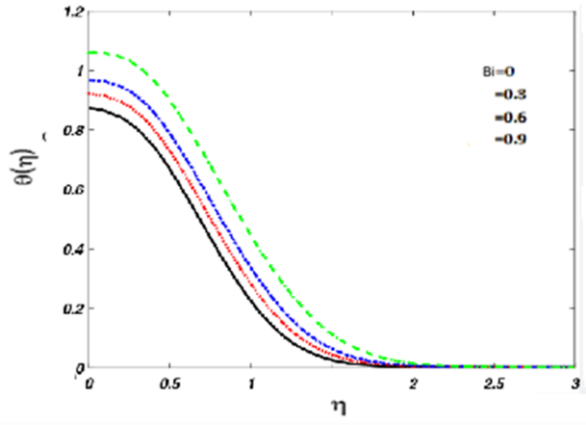

Fig. 5. Influence of Biot number on temperature.

Fig 6 highlights the impact of the space-dependent heat generation/absorption parameter A* on the temperature distribution. The left graph shows the effect of positive values of A*, representing heat generation, while the right graph depicts the effect of negative values of A*, corresponding to heat absorption. It is on a par with the study conducted in [11]. It was found that the dispersion of heat exhaust energy causes the temperature gradient to be larger, enhancing the values of A^*. The effect of heat absorption or generation factor on temperature can be visualised in Fig. 7. The graphs show that an increase in values of B^* rises the values of the temperature gradient. It is also found that while assigning negative values to B^* there is more heat absorption and a decrease in value of temperature gradient.

The result matches with outcomes of study conducted in [12]. The comparison of present results with Shah et al. [17] is presented in Fig 8. The results obtained are comparable and show an acceptable level of agreement.

4. Conclusions

The current work concentrates on flow simulation of copper carrying nanofluids along an elongated surface with varying width in association with electromagnetohydrodynamic (EMHD)

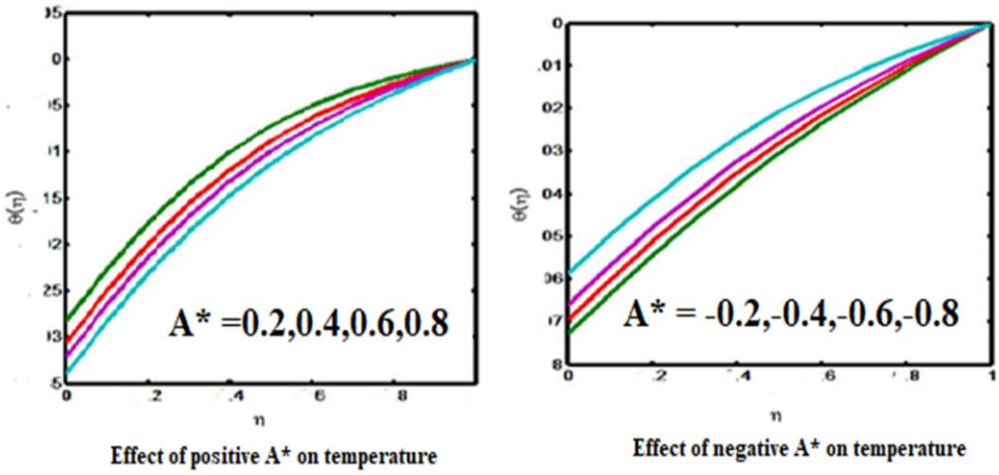

Fig. 6. The effect of heat absorption and generation factor on the temperature distribution.

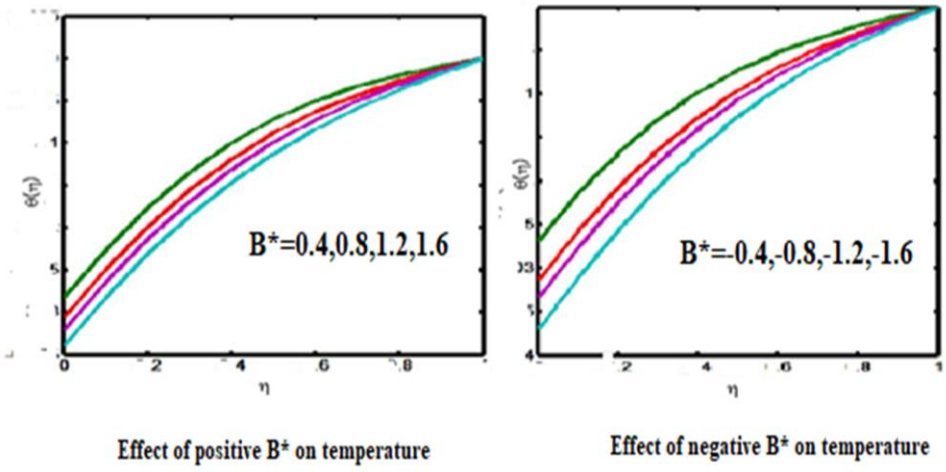

Fig. 7. Effect of positive and negative values of the space-dependent parameter on the temperature distribution.

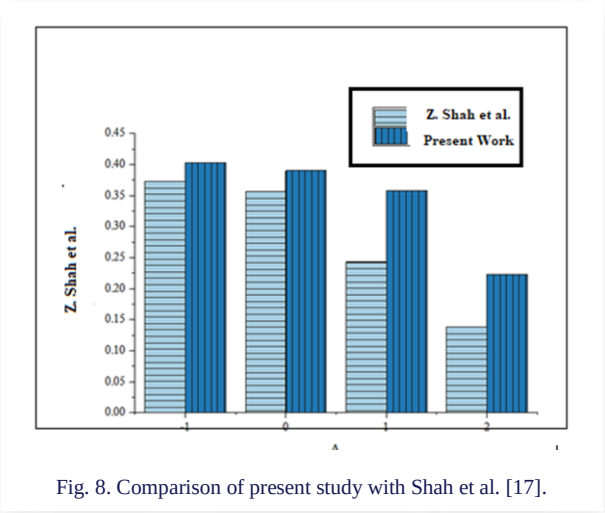

Fig. 8. Comparison of present study with Shah et al. [17].

flow. It also incorporates the heat flux with radiation phenomenon, which have a favourable effect on the flow behaviour. A survey has been conducted on the effects of an electrically charged particle-filled magnetic field on heat flux values, fluid with varied viscosity, and so on an extended surface with varying thickness. Diagrammatic representations of the temperature and velocity profiles are employed to analyse the influence of various physical parameters. The key findings from this investigation are summarized as follows:

- The comparative study of the obtained results using the Adams-Bashforth method with earlier investigation holds a good agreement, and also constitutes a validation of the proposed methodology;
- The temperature profile becomes more noticeable for the enhanced radiation parameters, nanoparticle fraction, and Eckert number; however, the opposite pattern is noticed for the increasing stretching parameter and Prandtl number;
- The increase in nanoparticle concentration, in association with the nonlinear stretching factor, reduces the nanofluid velocity;
- There is a noticeable reduction in the shear rate coefficient noticed for the increasing particle concentration, while it overshoots the heat transfer rate;
- While the power index of velocity term increases, both the nanofluid velocity and the nanofluid temperature also increase;
- Due to an increase in the boundary thickness factor, both the temperature as well as velocity of the fluid decrease;
- For increasing positive values, the time-dependent and space-dependent heat generation/absorption parameter contributes to heat generation, thereby increasing the temperature. Conversely, increasing the magnitude of negative values enhances heat absorption, which reduces the temperature.

The novelty of the present study is that it not only illustrates the physical properties of the parameters under conditions, but also provides a base for future research by associating the momentous role of magnetic and electric fields in customizing fluid velocity, which can be favourable for industrial sector dealing with stretching sheets. Further investigations using different concentrations, will be helpful in producing a finished product of the desired quality. The key points of this research can be successfully applied for further scientific investigation using stretching sheets.

References

[1] Khan, W.A., & Pop, I. (2010). Boundary-layer flow of a nanofluid past a stretching sheet. *International Journal of Heat and Mass Transfer*, 53(11-12), 2477–2483. doi: 10.1016/j.ijheatmasstransfer.2010.01.032

[2] Ibrahim, W., & Shankar, B. (2013). MHD boundary layer flow and heat transfer of a nanofluid past a permeable stretching sheet with velocity, thermal and solutal slip boundary conditions. *Computers & Fluids*, 75, 1−10. doi: 10.1016/j.compfluid.2013.01.014

[3] Gireesha, B., Sowmya, G., Khan, M.I., & Öztop, H.F. (2020). Flow of hybrid nanofluid across a permeable longitudinal moving fin along with thermal radiation and natural convection. *Computer methods and programs in biomedicine*, 185, 105166. doi: 10.1016/j.cmpb.2019.105166

[4] Makarem, M.A., Bakhtyari, A., & Rahimpour, M.R. (2018). A numerical investigation on the heat and fluid flow of various nanofluids on a stretching sheet. *Heat Transfer – Asian Research*, 47(2), 347–365. doi: 10.1002/htj.21307

[5] Ghalambaz, M., Groşan, T., & Pop, I. (2019). Mixed convection boundary layer flow and heat transfer over a vertical plate embedded in a porous medium filled with a suspension of nano-encapsulated phase change materials. *Journal of Molecular Liquids*, 293, 111432. doi: 10.1016/j.molliq.2019.111432

[6] Hajjar, A., Mehryan, S., & Ghalambaz, M. (2020). Time periodic natural convection heat transfer in a nano-encapsulated phase-change suspension. *International Journal of Mechanical Sciences*, 166, 105243. doi: 10.1016/j.ijmecsci.2019.105243

[7] Saeed, A., Kumam, P., Nasir, S., Gul, T., & Kumam, W. (2021). Non-linear convective flow of the thin film nanofluid over an inclined stretching surface. *Scientific Reports*, 11, 18410. doi: 10.1038/s41598-021-97576-x

[8] Mathew, A., Areekara, S., Sabu, A., & Saleem, S. (2021). Significance of multiple slip and nanoparticle shape on stagnation point flow of silver-blood nanofluid in the presence of induced magnetic field. *Surfaces and Interfaces*, 25, 101267. doi: 10.1016/j.surfin.2021.101267

[9] Krishnamurthy, M., Prasanna Kumara, B., Gireesha, B., & Gorla, R.S. (2015). Effect of viscous dissipation on hydromagnetic fluid flow and heat transfer of nanofluid over an exponentially stretching sheet with fluid-particle suspension. *Cogent Mathematics*, 2, 1050973. doi: 10.1080/23311835.2015.1050973

[10] Senthilraja, S., Vijayakumar, K., & Gangadevi, R. (2015). A comparative study on thermal conductivity of Al_2O_3/water, CuO/water and Al_2O_3–CuO/water nanofluids. *Digest Journal of Nanomaterials and Biostructures*, 10(4), 1449–1458.

[11] Chamkha, A., Doostanidezfuli, A., Izadpanahi, E., & Ghalambaz, M. (2017). Phase-change heat transfer of single/hybrid nanoparticles-enhanced phase-change materials over a heated horizontal cylinder confined in a square cavity. *Advanced Powder Technology*, 28(2), 385–397. doi: 10.1016/j.apt.2016.10.009

[12] Sharma, K., & Kumar, S. (2023). Impacts of low oscillating magnetic field on ferrofluid flow over upward/downward moving rotating disk with effects of nanoparticle diameter and nanolayer. *Journal of Magnetism and Magnetic Materials*, 575, 170720. doi: 10.1016/j.jmmm.2023.170720.

[13] Gopal, D., Saleem, S., Jagadha, S., Ahmad, A., Almatroud, A.O., & Kishan, N. (2021). Numerical analysis of higher order chemical reaction on electrically MHD nanofluid under influence of viscous dissipation. *Alexandria Engineering Journal*, 60(1), 1861–1871. doi: 10.1016/j.aej.2020.11.034

[14] Sowmya, G., Gireesha, B.J., & Madhu, M. (2020). Analysis of a fully wetted moving fin with temperature-dependent internal heat generation using the finite element method. *Heat Transfer*, 49(4), 1939–1954. doi: 10.1002/htj.21701

[15] Alsaedi, A., Hayat, T., Qayyum, S., & Yaqoob, R. (2020). Eyring-Powell nanofluid flow with nonlinear mixed convection: Entropy generation minimization. *Computer Methods and Programs in Biomedicine*, 186, 105183. doi: /10.1016/j.cmpb.2019.105183

[16] Fang, T., Zhang, J., & Zhong, Y. (2012). Boundary layer flow over a stretching sheet with variable thickness. *Applied Mathematics and Computation*, 218(13), 7241–7252. doi: 10.1016/j.amc.2011.12.094

[17] Shah, Z., Ramzan, M., Kumam, P., Khan, W., Watthayu, W., & Kumam, W. (2022). Bidirectional flow of MHD nanofluid with Hall current Cattaneo-Christove heat flux towards the stretching sheet. *Plos One*, 17(4), e0264208. doi: 10.1371/journal.pone.0264208

[18] Khader, M.M., & Megahed, A.M. (2013). Numerical solution for boundary layer flow due to a nonlinearly stretching sheet with variable thickness and slip velocity. *The European Physical Journal Plus*, 128, 100. doi: 10.1140/epjp/i2013-13100-7

[19] Alawi, O.A., Sidik, N.A.C., Xian, H.W., Kean, T.H., & Kazi, S.N. (2018). Thermal conductivity and viscosity models of metallic oxides nanofluids. *International Journal of Heat and Mass Transfer*, 116, 1314–1325. doi: 10.1016/j.ijheatmasstransfer.2017.09.133

[20] Suresh, S., Venkitaraj, K.P., Selvakumar, P., & Chandrasekar, M. (2012). Effect of Al_2O_3–Cu/water hybrid nanofluid in heat transfer. *Experimental Thermal and Fluid Science*, 38, 54–60. doi: 10.1016/j.expthermflusci.2011.11.007

[21] Momin, G.C. (2013). Experimental investigation of mixed convection with water-Al_2O_3 & hybrid nanofluid in inclined tube for laminar flow. *International Journal of Scientific and Technology Research*, 2(12), 195–202.

[22] Takabi, B., & Salehi, S. (2014). Augmentation of the heat transfer performance of a sinusoidal corrugated enclosure by employing hybrid nanofluid. *Advances in Mechanical Engineering*, 6, 147059. doi: 10.1155/2014/147059

[23] Devi, S.P.A., & Devi, S.S.U. (2016). Numerical investigation of hydromagnetic hybrid Cu–Al_2O_3/water nanofluid flow over a permeable stretching sheet with suction. *International Journal of Nonlinear Sciences and Numerical Simulation*, 17(5), 249–257. doi: 10.1515/ijnsns-2016-0037

[24] Ghalambaz, M., Doostani, A., Izadpanahi, E., & Chamkha, A. (2017). Phase-change heat transfer in a cavity heated from below: The effect of utilizing single or hybrid nanoparticles as additives. *Journal of the Taiwan Institute of Chemical Engineers*, 72, 104–115. doi: 10.1016/j.jtice.2017.01.010

[25] Shuguang, Li., Puneet, V., Saeed, A.M., Singhal, A., Fuad, A.M., Yarimi, Al., & Ijaz Khan, M. (2024). Analysis of the Thomson and Troian velocity slip for the flow of ternary nanofluid past a stretching sheet. *Scientific Reports*, 14(1), 2340−2351. doi: 10.1038/s41598-024-83032-z

[26] Prajapati, V.J., & Meher, R. (2024). Analysis of MHD tangent hyperbolic hybrid nanofluid flow with different base fluids over a porous stretched sheet. *Journal of Taibah University for Science*, 18(1), 2300851. doi: 10.1080/16583655.2023.2300851

[27] Khan, M.S., Ahmad, S., Shah, Z., Vrinceanu, N., Mansoor, H., & Alshehri, M. (2024). Natural convection heat transfer of a hybrid nanofluid in a permeable quadrantal enclosure with heat generation. *Case Studies in Thermal Engineering*, 56, 104207. doi: 10.1016/j.csite.2024.104207.

[28] Alsabery, A.I., Armaghani, T., Chamkha, A.J., & Hashim, I. (2020). Two-phase nanofluid model and magnetic field effects on mixed convection in a lid-driven cavity containing heated triangular wall. *Alexandria Engineering Journal*, 59(1), 129−148. doi: 10.1016/j.aej.2019.12.017.

[29] Jameel, M., Shah, Z., Shafiq, A., Rooman, M., Vrinceanu, N., Alshehri, A., & Islam, S. (2023). Statistical and entropy optimization modeling for radiative hybrid nanofluid flow with Hall effect over exponential stretching/shrinking plate. *International Journal of Thermofluids*, 20, 100398. doi: 10.1016/j.ijft.2023.100398

[30] Shah, Z., Sulaiman, M., Dawar, A., Alshehri, M.H., & Vrinceanu, N. (2024). Darcy-Forchheimer MHD rotationally symmetric micropolar hybrid-nanofluid flow with melting heat transfer over a radially stretchable porous rotating disk. *Journal of Thermal Analysis and Calorimetry*, 149, 14625–14641, doi: 10.1007/s10973-024-12986-z

[31] Muhammad, K., Abdelmohsen, S.A., Abdelbacki, A.M., & Ahmed, B. (2022). Darcy-Forchheimer flow of hybrid nanofluid subject to melting heat: A comparative numerical study via shooting method. *International Communications in Heat and Mass Transfer*, 135, 106160. doi: 10.1016/j.icheatmasstransfer.2022.106160

[32] Shah, Z., Sulaiman, M., Khan, W., Vrinceanu, N., & Alshehri, M.H. (2024). Gyrotactic microorganism's and heat transfer analysis of water conveying MHD SWCNT nanoparticles using fourth-grade fluid model over Riga plate. *Case Studies in Thermal Engineering*, 55, 104119. doi: 10.1016/j.csite.2024.104119

[33] Adel, M., Khader, M.M., & Ahmad, H. (2024). MHD nanofluid flow and heat transfer caused by a stretching sheet that is heated convectively: an approximate solution using ADM. *Case Studies in Thermal Engineering*, 60, 104683. doi: /10.1016/j.csite.2024.104683

[34] Brinkman, H.C. (1952). The viscosity of concentrated suspensions and solutions. *Journal of Chemical Physics*, 20(4), 571−571. doi: 10.1063/1.1700493